Comparison of Three Popular Control Strategies Used in Shunt Active Power Filters

Anant Naik
Research Scholar, EEE Department
NITK Surathkal
Karnataka INDIA
anantnaik05@gmail.com

Udaykumar Yaragatti
member IEEE,EEE Department
NITK Surathkal
Karnataka INDIA

Abstract— **Active power filtering has gained more importance in the power quality arena as it gives best solution for all power quality issues. Shunt active power filtering is effective and the performance of such units largely depends upon the control strategies used for reference current generation. There are different techniques used for this. Here an attempt is made to compare three major methods used for generation of reference current. The results are obtained using these three methods for the same system under balanced and unbalanced supply voltage conditions. Matlab/Simulink is used to model and simulate the various components of the systems.**

Keywords—SAPF (shunt active power filters), CC-VSI (current controlled voltage source inverter), IRPT (instantaneous reactive power theory), SRF (synchronous reference frame), indirect power control.

I. INTRODUCTION

The numerous power quality PQ problems in the electric power networks are due to the increased use of power semiconductor devices in wide variety of loads. With the development of power electronics devices, the non linear loads that consume non sinusoidal current have increased significantly e.g. VFD, electronic fan regulator, UPS, electronic choke fitted fluorescent lamps etc. These types of equipments behave as non linear loads and draw harmonic current from the power network. The non sinusoidal voltage and/or current have adverse effect on the utilities and the load connected to it [1]. Hence it has become very essential to pay attention to the power quality issues. Several power quality standards are defined in order to keep the harmonic distortion within the limits like IEEE-519-1992/IEC 61000 [2]. The methods used to suppress/eliminate harmonics include passive power filtering and active power filtering. The conventional passive filters suffer from drawbacks such as huge size, resonance problems, dependency on source impedance and fixed compensation [3]. Active power filtering uses either a current source inverter or a voltage source inverter which acts as a harmonic source to compensate for the load harmonics. APFs are capable enough to provide the solution related to harmonic compensation, reactive power compensation, balancing three-phase line currents, damping of oscillation in currents and voltage regulation [4].

The shunt APF has to generate a current signal such that the load harmonic and reactive power components are fed from VSI and the source is free from it. The accuracy and fast response of APF controller depend upon the proper estimation of reference current and the hardware, both in quality and configuration. Some direct and indirect controls of shunt APFs are also reported in the literature [5], [6]. The most widely used control methods are instantaneous- pq theory by Akagi [7] and the synchronous reference frame method [8].Another very popular method includes indirect power control method is used in [9].

In this paper, these three control techniques are compared for a given system under both sinusoidal and non-sinusoidal supply voltage conditions. Simulations are carried using MATLAB/Simulink tool. Section II covers brief theory of these three control strategies. The system considered for the study is described in section III and the results obtained for different conditions by these three methods are given in section IV.

II. VARIOUS CONTROL STRATEGIES

A. Instantaneous Reactive Power Theory

Akagi et al. [7] proposed a concept based on the theory of instantaneous reactive power in the *α-β* reference frame; this theory stimulates the realization of three phase, three-wire APFs. In this theory, the instantaneous source voltage and current signals in *a-b-c* coordinates are transformed into two-phases *i.e. α-β* orthogonal coordinates as follows.

$$\begin{bmatrix} V_{s\alpha} \\ V_{s\beta} \end{bmatrix} = \sqrt{\frac{2}{3}} \begin{bmatrix} 1 & -\frac{1}{2} & -\frac{1}{2} \\ 0 & \frac{\sqrt{3}}{2} & -\frac{\sqrt{3}}{2} \end{bmatrix} \begin{bmatrix} V_{sa} \\ V_{sb} \\ V_{sc} \end{bmatrix} \quad (1)$$

$$\begin{bmatrix} i_{L\alpha} \\ i_{L\beta} \end{bmatrix} = \sqrt{\frac{2}{3}} \begin{bmatrix} 1 & -\frac{1}{2} & -\frac{1}{2} \\ 0 & \frac{\sqrt{3}}{2} & -\frac{\sqrt{3}}{2} \end{bmatrix} \begin{bmatrix} i_{La} \\ i_{Lb} \\ i_{Lc} \end{bmatrix} \quad (2)$$

For simplicity, the zero-phase sequence component voltage and current signals are eliminated in (1) and (2). The instantaneous active power (p) and the instantaneous imaginary power (q) in a three-phase circuit are defined in (3).

$$\begin{bmatrix} p \\ q \end{bmatrix} = \begin{bmatrix} V_{s\alpha} & V_{s\beta} \\ -V_{s\beta} & V_{s\alpha} \end{bmatrix} \begin{bmatrix} i_{L\alpha} \\ i_{L\beta} \end{bmatrix} \quad (3)$$

Using (3) load current in α-*β* frame can be calculated as:

$$\begin{bmatrix} i_{L\alpha} \\ i_{L\beta} \end{bmatrix} = \frac{1}{V_{s\alpha}^2 + V_{s\beta}^2} \begin{bmatrix} V_{s\alpha} & V_{s\beta} \\ -V_{s\beta} & V_{s\alpha} \end{bmatrix} \begin{bmatrix} p \\ q \end{bmatrix} \quad (4)$$

The block diagram of this method is as shown in figure (1). The reference compensating current can be calculated in such a way that it supplies the instantaneous reactive power (*q*) and the harmonic component of the instantaneous active power (p~). The reference compensating current (i_c^*) can be obtained as:

$$\begin{bmatrix} i^*_{c\alpha} \\ i^*_{c\beta} \end{bmatrix} = \frac{1}{V_{s\alpha}^2 + V_{s\beta}^2} \begin{bmatrix} V_{s\alpha} & V_{s\beta} \\ -V_{s\beta} & V_{s\alpha} \end{bmatrix} \begin{bmatrix} \tilde{p} \\ q \end{bmatrix} \quad (5)$$

The compensating current signals in *α-β* frame can be transferred to *a-b-c* frame using inverse Clark's transformation as:

$$\begin{bmatrix} i^*_{ca} \\ i^*_{cb} \\ i^*_{cc} \end{bmatrix} = \sqrt{\frac{2}{3}} \begin{bmatrix} 1 & 0 \\ -\frac{1}{2} & \frac{\sqrt{3}}{2} \\ -\frac{1}{2} & -\frac{\sqrt{3}}{2} \end{bmatrix} \begin{bmatrix} i^*_{c\alpha} \\ i^*_{c\beta} \end{bmatrix} \quad (6)$$

This method does not take into account the zero sequence components, and hence, the effect of unbalanced voltages and currents. The instantaneous reactive power (*p-q*) theory is widely used for three-phase balanced non-linear loads, such as rectifiers.

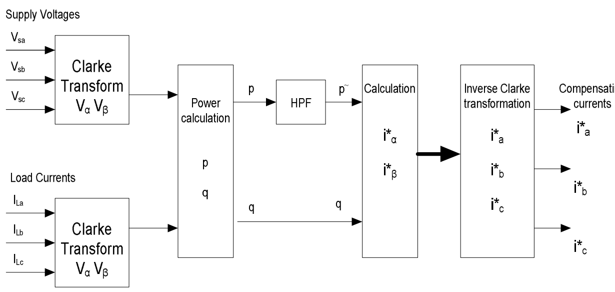

Figure 1: Block diagram of the instantaneous reactive power theory.

B. Synchronous Reference Frame

The active power filter control algorithm, based on synchronous reference frame (SRF) method [8], relies on Clarke's and Park's transformations, as shown in figure(2). In this method, the load current signals are first transformed into synchronous reference (*dq0*) frame. The fundamental component of the load current after transformation is a DC value and the harmonics appear like a ripple over this DC offset. A low pass filter is used to separate harmonic components from the load current. The active power loss component is subtracted from this current to get the reference d and q component of filter currents. Then reference current in abc frame is obtained using inverse transformation. The reference current is compared with actual filter current and the error current is used by the hysteresis controller to generate the pulses. In general the rotating frame dq0 is obtained from abc quantities by the following transformation.

$$\begin{bmatrix} x_0 \\ x_d \\ x_q \end{bmatrix} = \sqrt{\frac{2}{3}} \begin{bmatrix} \frac{1}{\sqrt{2}} & \frac{1}{\sqrt{2}} & \frac{1}{\sqrt{2}} \\ \cos\theta & \cos(\theta - \frac{2\pi}{3}) & \cos(\theta + \frac{2\pi}{3}) \\ \sin\theta & \sin(\theta - \frac{2\pi}{3}) & \sin(\theta + \frac{2\pi}{3}) \end{bmatrix} \begin{bmatrix} x_a \\ x_b \\ x_c \end{bmatrix} \quad (7)$$

For synchronization a PLL is used which derives phase angle *θ* the AC supply voltage.

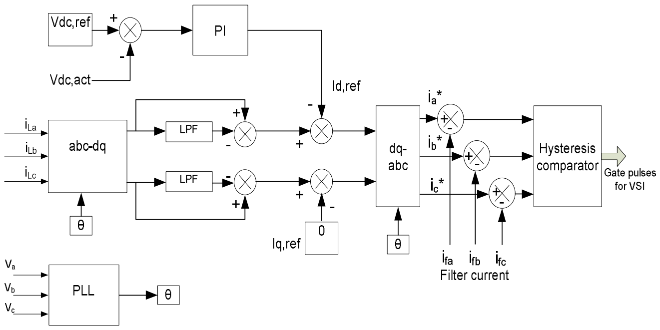

Figure 2: Block diagram of SRF method.

C. Indirect power control method

The instantaneous source voltage of any one phase (phase-*a* in this work) v_{sa}, actual DC-bus capacitor voltage V_{dc} and the actual instantaneous source currents (i_{sa}, i_{sb}, i_{sc}) are the main inputs to the algorithm. To maintain a constant DC-bus capacitor voltage in the CC-VSI, the error $V_e(k)$ between the square values of reference DC-bus capacitor voltage and actual DC-bus capacitor voltage at the *k*th sampling instant is computed as:

$$V_e(k) = V^2_{dcref} - V^2_{dc}(k) \quad (8)$$

where, V_{dcref} is the reference DC-bus capacitor voltage and $V_{dc}(k)$ is the actual DC-bus capacitor voltage at *k*th sampling instant. This DC-bus capacitor voltage error is processed through a PI controller. The output of the controller is considered as peak value I_{sm} of source currents at every sample which has two components. One of them is the fundamental active component of load current and the other is loss component of the inverter circuit.

The output of the controller at k^{th} sampling instant in discrete system is given as:

$$I_{sm}(k) = K_{ep} V_e(k) + I_{sm}(k-1) \quad (9)$$

where, K_{ep} is the gain of the controller and $I_{sm}(k)$ and $I_{sm}(k\text{-}1)$ are the output of the controller at k^{th} and $(k\text{-}1)^{th}$ sampling instant, respectively. In the discrete system equation (9) can be written by taking its z transform as:

$$I_{sm}(z) = K_{ep} V_e(z) + z^{-1} I_{sm}(z) \quad (10)$$

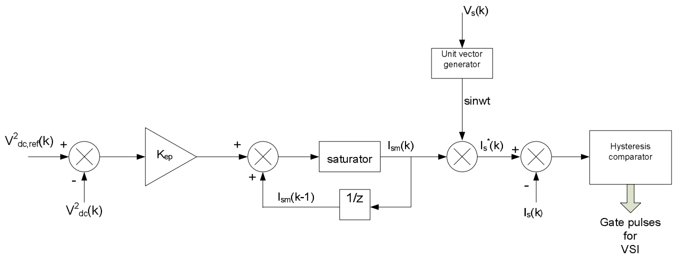

Figure 3: Control circuit

III. SYSTEM DESCRIPTION

All the three above mentioned control techniques are implemented for a common system that is represented in figure (4). Here a three phase supply is used to feed a non- linear load consisting of a diode bridge rectifier feeding RL load at its DC side. At PCC, a current controlled voltage source inverter (CC-VSI) is acting as SAPF. The DC side capacitor and AC side inductance of this VSI acts as filter components. The gate pulses to the inverter are generated by an hysteresis type pulse generator. The heart of APF is the reference current generator block. This unit takes voltage and/or current from the supply and/or load to generate the reference current depending upon the type of control strategy used.

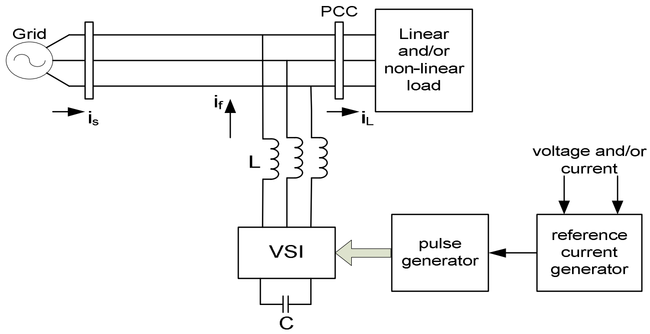

Figure 4: System description

IV. RESULTS AND DISCUSSIONS

The system is simulated under two different conditions viz balanced and unbalanced system voltages. In both the cases load current, source current and the filter current are measured before and after the addition of APF. At t=0.1sec filter is added and the simulation is run for 0.4 sec. The source current THDi before and after the addition of filter is also observed. The three different control strategies offer different performance and is summarized in the Table 1 given below. The other important parameters to be considered while selecting the control strategy for APF is given in Table 2.

TABLE 1: PERFORMANCE OF THREE DIFFERENT CONTROL STRATEGIES

System/supply voltage	Parameter	pq control	dq control	Indirect power control
Balanced voltage	Load current THD	20.53	20.49	20.54
	Source current THD (after filtering)	1.74	3.29	1.95
	Displacement power factor	Near unity	Poor	Near unity
Unbalanced voltage	Load current THD	21.29	21.22	22.69
	Source current THD (after filtering)	25.13	5.14	1.8
	Displacement power factor	Poor	Poor	Near unity

TABLE 2: PARAMETER COMPARISON IN THREE DIFFERENT CONTROL STRATEGIES

Parameter	pq control	dq control	Indirect power control
No. of conversions	three	two	nil
No. of input signals(sensors) required	two	three	three
PLL requirement	no	yes	yes
Complexity in digital implementation	more	more	less

A. *Case (A): Balanced Supply Voltage Case:*

1) pq method:

Figure (5) shows the currents at different nodes when the system voltage is balanced. The source power factor is llustrated in figure (6).The load current and source current THDi is shown in figure 7 (a) and (b) respectively.

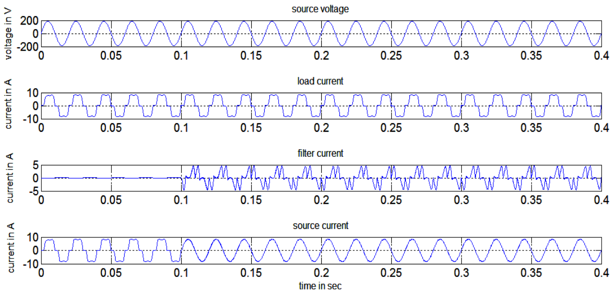

Figure 5: pq method (balanced supply): Currents at different nodes

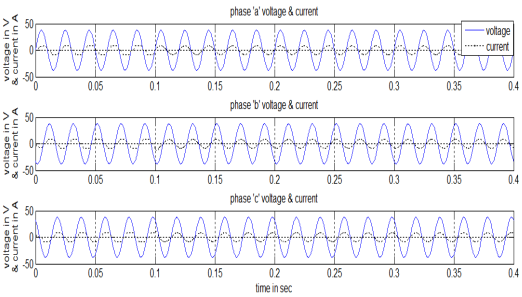

Figure 6: pq method (balanced supply): Source voltage and current in three phases.

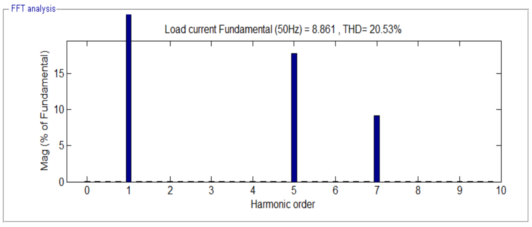

(a)

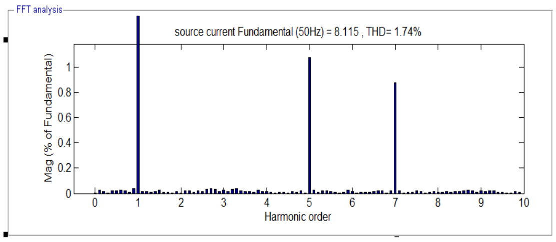

(b)

Figure 7: pq method (balanced supply): Load current and source current THDi

2) dq method:

Figure (8) shows the currents at different nodes when the system voltage is balanced. The source power factor is illustrated in figure (9).The load current and source current THDi is shown in figure 10 (a) and (b) respectively.

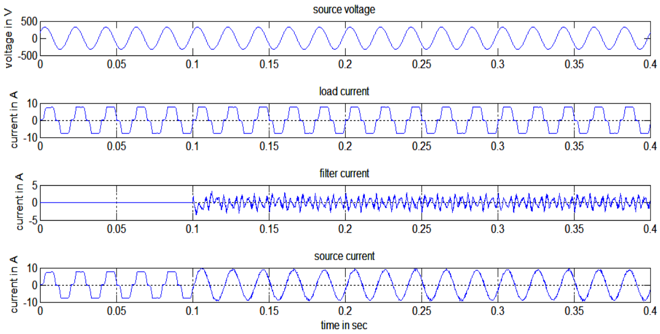

Figure 8: dq method (balanced supply): Currents at different nodes

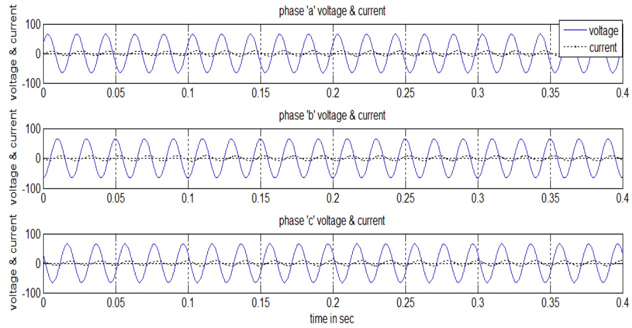

Figure 9: dq method (balanced supply): Source voltage and current in three phases

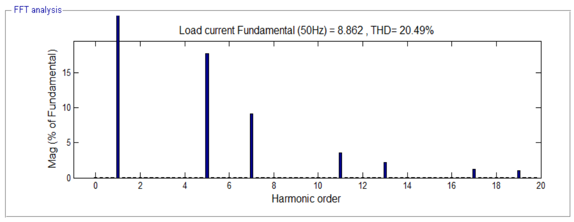

(a)

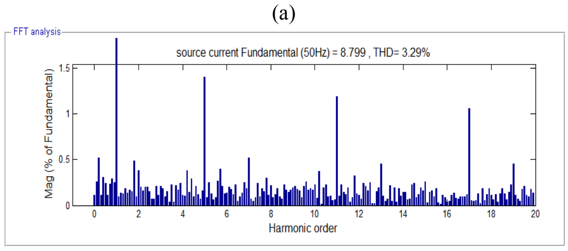

(b)

Figure 10: dq method (balanced supply): Load current and source current THDi

3) Indirect Power:

Figure (11) shows the currents at different nodes when the system voltage is balanced. The source power factor is illustrated in figure (12).The load current and source current THDi is shown in figure 13 (a) and (b) respectively.

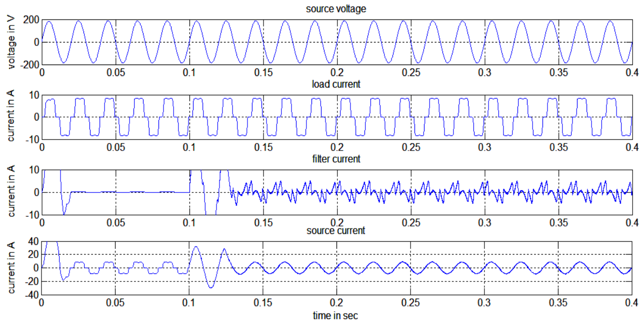

Figure 11: indirect power method (balanced supply): Currents at different nodes

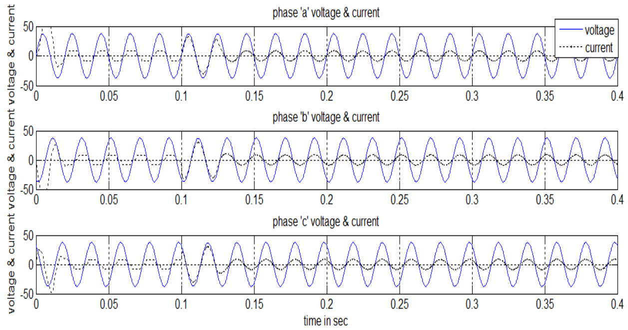

Figure 121: indirect power method (balanced supply): Source voltage and current in three phases

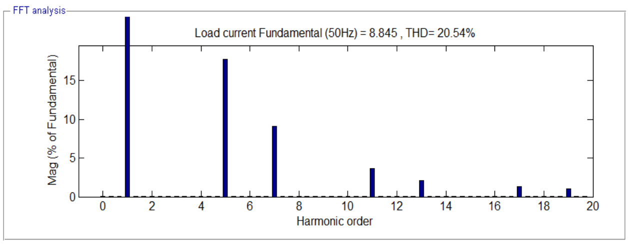

(a)

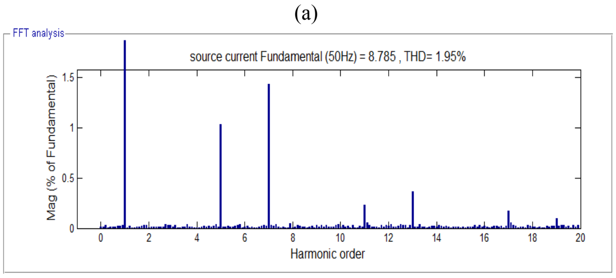

(b)

Figure 132: indirect power method (balanced supply): Load current and source current THD

B. Case B: Unbalanced Supply Voltage Case:

Now the supply voltage is made polluted with the introduction of 5th and 7th harmonic components.

1) pq method:

Figure (14) shows the currents at different nodes when the system voltage is unbalanced. The source power factor is illustrated in figure (15).The supply voltage, load current and source current THDi is shown in figure 16(a), (b) and (c) respectively.

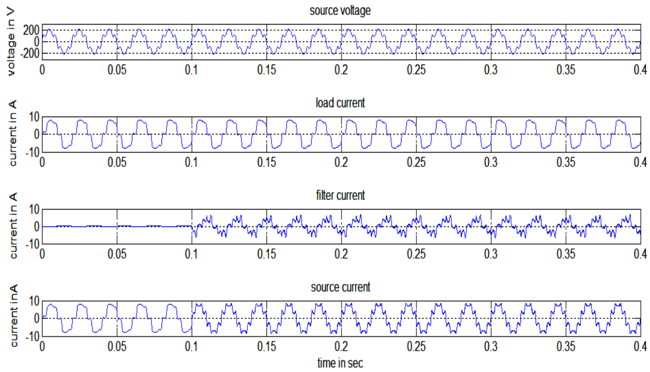

Figure 14: pq method (unbalanced supply): Currents at different nodes

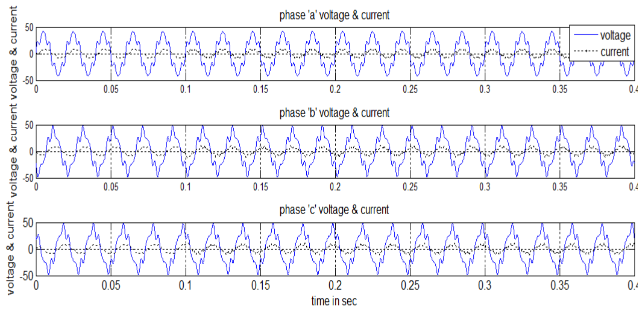

Figure 15: pq method (unbalanced supply): Source voltage and current in three phases

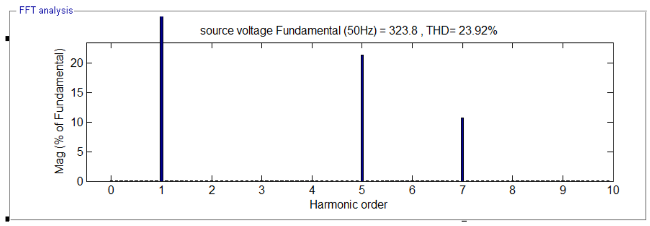

(a)

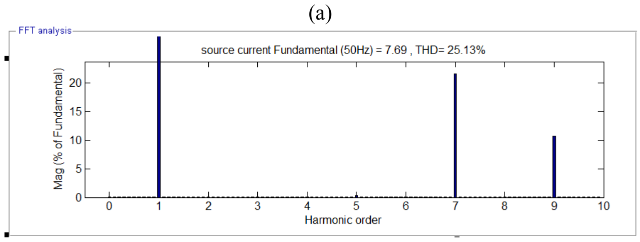

(b)

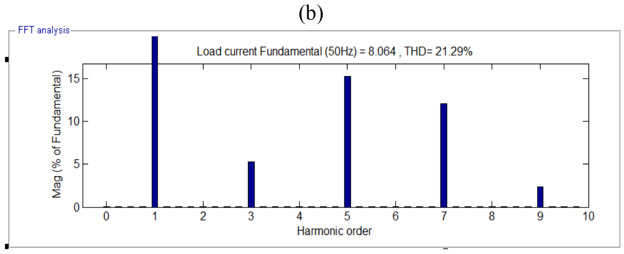

(c)

Figure 16: pq method (unbalanced supply): source voltage, load current and source current THD

2) dq method:

Figure (17) shows the currents at different nodes when the system voltage is unbalanced. The source power factor is illustrated in figure (18).The supply voltage, load current and source current THD is shown in figure 19(a), (b) and (c) respectively.

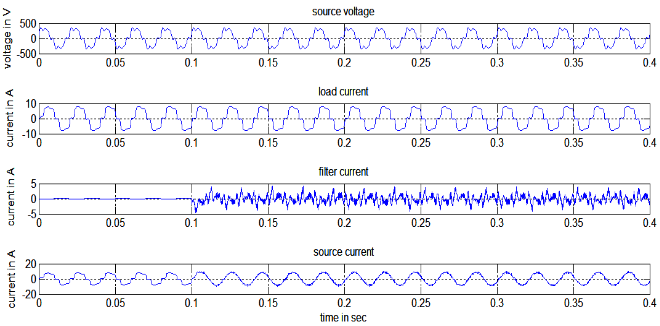

Figure 17: dq method (unbalanced supply): Currents at different nodes

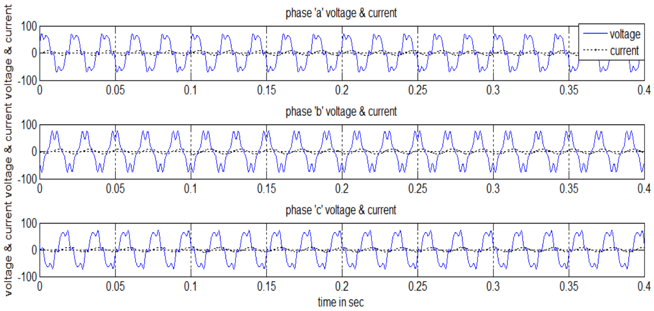

Figure 18: dq method (unbalanced supply): Source voltage and current in three phases

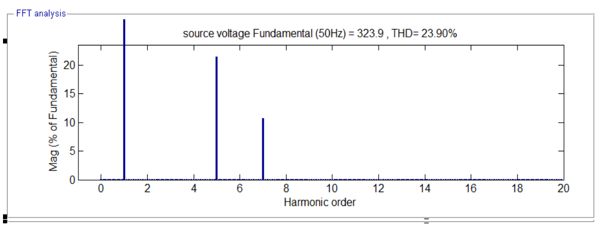

(a)

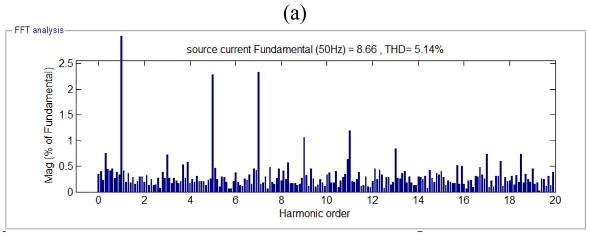

(b)

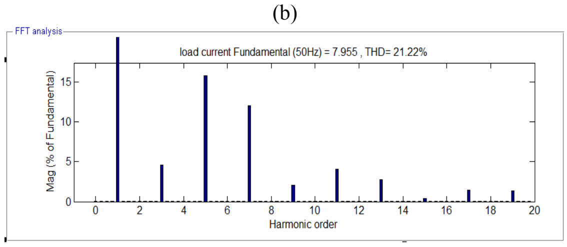

(c)

Figure 19: dq method (unbalanced supply): source voltage, load current and source current THD

3) Indirect Power:

Figure (20) shows the currents at different nodes when the system voltage is unbalanced. The source power factor is illustrated in figure (21).The supply voltage, load current and source current THD is shown in figure 22(a), (b) and (c) respectively.

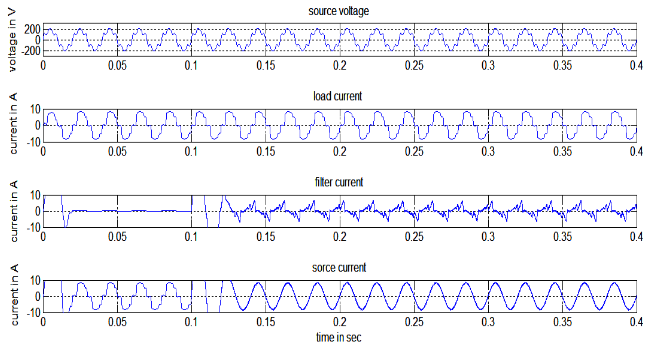

Figure 20: indirect power method (unbalanced supply): Currents at different nodes

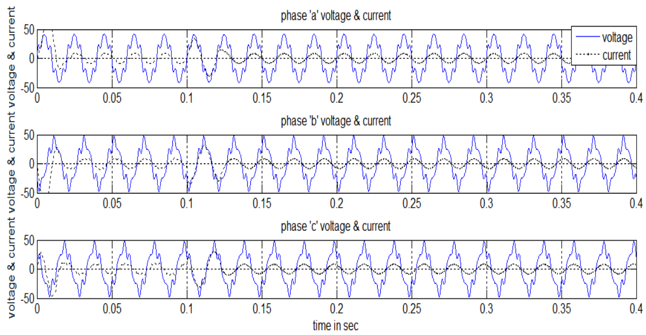

Figure 21: indirect power method (unbalanced supply): Source voltage and current in three phases

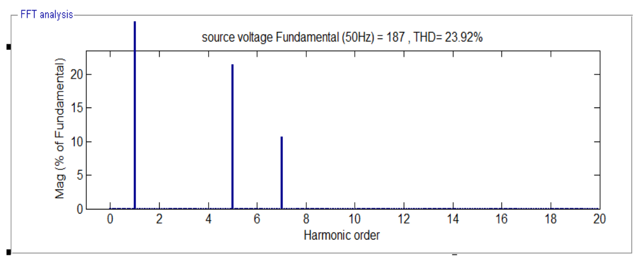

(a)

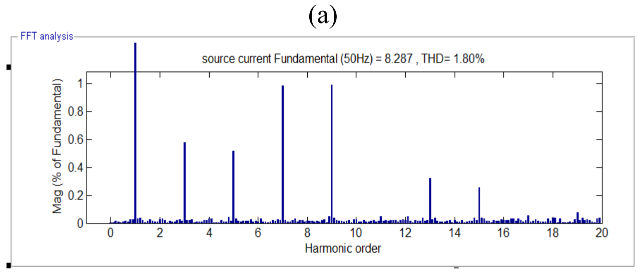

(b)

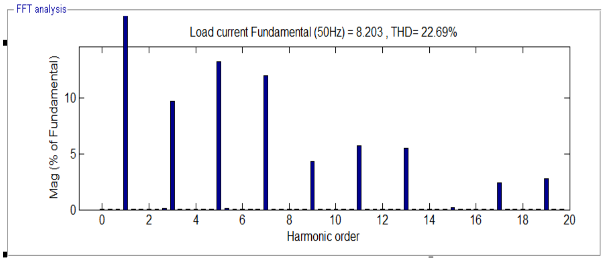

(c)

Figure 22: indirect power (unbalanced supply): source voltage, load current and source current THD

V. CONCLUSIONS

The three main control strategies used in SAPF simulated for balanced and unbalanced system conditions. It is observed that the indirect power control strategy is a better option as it works satisfactorily in both the cases. Also the circuit complexities are less and the digital implementation is simpler as less no of signals are required. It is also observed that the displacement power factor in this method is always near unity.

REFERENCES

[1] A report by load characteristics task force and effects of harmonics task force, "The effects of power system harmonics on power system equipment and loads," *IEEE Transaction on PAS*, Vol. 104, No. 9, September, 1998.

[2] IEEE Recommended Practice for Monitoring Electric Power Quality, IEEE Std. 1 159- 1995.

[3] D. E. Steeper and R. P. Stratford, "Reactive compensation, harmonic suppression for industrial power systems using thyristor converters," *IEEE Transactions on Industrial Applications*, Vol.12, No. 3, May/June 1976, pp. 232-254.

[4] B. Singh, K. Al-Haddad, and A. Chandra, "A review of active power filters for power quality improvement," *IEEE Transaction on Industrial Electronics*, vol. 46, no.5, pp. 960-971, October 1999 .

[5] A. Chandra, B. Singh, B. N. Singh, and K. Al-Haddad, "An improved control algorithm of shunt active filter for voltage regulation, harmonic elimination, power-factor correction, and balancing of nonlinear loads," IEEE Transactions on Power Electronics, vol.15, no. 3, pp. 495-507, May 2000

[6] B. Singh, and V. Verma, "An indirect current control of hybrid power filter for varying loads," IEEE Transactions on Power Delivery, vol. 21, no.1, pp. 178-184, January 2006.

[7] H. Akagi, Y. Kanazawa and A.Nabae, "Instantaneous reactive power compensators comprising switching devices without energy storage components," *IEEE Trans, Ind. Appl.,* vol. IA-20,no.3,pp.625-630,May/June 1984.

[8] A. Nabae and T. Tanaka," A new definition of instantaneous active-reactive current and a power based on instantaneous space vectors on polar coordinates in three phase circuits," *IEEE Tran. Power Delivery*, vol. 11, no.3, pp. 1238-1243, Jul.1996.

[9] Patidar R. D., and Singh, S. P., "Digital signal processor based shunt active filter controller for customer-generated harmonics and reactive power compensation." *Electric Power Components and Systems*, Vol. 38, pp. 937-959. 2010.